UAV-Aided Calibration for Commissioning of Phased Array Radio Telescopes

Stefan J. Wijnholds
R&D Department
ASTRON
Dwingeloo, The Netherlands
wijnholds@astron.nl

Giuseppe Pupillo
Instituto di Radioastronomia
INAF
Bologna, Italy
g.pupillo@ira.inaf.it

Pietro Bolli
Arcetri Astrophysical Observatory
INAF
Florence, Italy
pbolli@arcetri.inaf.it

Giuseppe Virone
IEIIT
CNR
Turin, Italy
giuseppe.virone@ieiit.cnr.it

***Abstract*—Calibration of antenna positions and instrumental response is a crucial step in the commissioning of a phased array radio telescope. The Low Frequency Aperture Array system of the Square Kilometre Array (SKA) is envisaged to consist of about 131,000 antennas. In this paper, we propose a strategy to efficiently conduct commissioning calibration of such a large phased array radio telescope using a near-field probe mounted on an Unmanned Aerial Vehicle (UAV). We demonstrate the effectiveness of the proposed method using simulations. This indicates that potentially cost-saving relaxation of requirements on placement accuracy is possible. We also propose to validate this method in practice using the Low Frequency Array (LOFAR).**

I. Introduction

The radio astronomical community is currently making detailed plans for the Square Kilometre Array (SKA) [1]. The low frequency receiving system of the SKA (SKA-low) will be a phased array instrument operating in the 50 – 350 MHz frequency range consisting of 512 stations with 256 antennas each [2]. Due to the large fractional bandwidth, the antennas in a station will be placed in an irregular configuration. Such a configuration has the additional advantage that some additional randomisation of the antenna positions by a fast but inaccurate antenna installation procedure will not fundamentally change the performance of the instrument. A fast and simple installation procedure is attractive in view of the large number of antennas to be rolled out and the harsh working conditions in the Western Australian Desert. The downside of such an approach is, that the antenna positions are not accurately known at the start of the commissioning phase, which will put the SKA-low system at a more challenging starting position than current low frequency instruments such as the Low Frequency Array (LOFAR) [3] and the Murchison Widefield Array (MWA) [4], whose positions were very accurately known from the start.

Another issue is, that the element radiation patterns will be different for each element in an irregular array. This effect is hitherto ignored in LOFAR. Its effect on calibration solutions is so far remedied by averaging over time, but it was recently concluded that an improved beam model is required.

In this paper, we show how both issues (inaccurately known antenna positions and inaccurately known element radiation patterns) can be addressed using a probe mounted on an Unmanned Aerial Vehicle (UAV). Such an UAV system has been developed by a collaboration between CNR and INAF in Italy [5] and successfully demonstrated on a small testbed in Medicina [6]. With the methods proposed in this paper, such a system can aid the commissioning of future phased array radio telescopes, in particular the SKA-low system. We are currently making detailed plans to demonstrate the combination of the UAV measurement techniques described in [6] with the calibration scheme presented in this paper on LOFAR.

Notation Upper case bold symbols denote matrices, lower case bold symbols denote vectors and italic symbols denote scalars. Complex conjugation is denoted by $\bar{\cdot}$ (overbar), the inner product by $\cdot$, the transpose by ^{T}, the norm of a vector by $\|\cdot\|$ and the phase of a complex number by $\angle\cdot$.

II. Data model

For simplicity of presentation, we consider an array in which all antennas measure only a single polarisation. It will become apparent later that it is straightforward to extend our method to antenna systems measuring both polarisations. The UAV transmits a signal $s(t)$ that is assumed to be strong enough to ignore the presence of the astronomical sources inside the field of view of the antennas in the frequency channel in which the measurement is done. When the UAV is at position $\mathbf{x}_{\mathrm{UAV}}$, this signal arrives at the pth antenna at position $\mathbf{x}_p$ with phase $2\pi \|\mathbf{x}_{\mathrm{UAV}} - \mathbf{x}_p\| / \lambda$ and an amplitude that depends on path loss, polarisation mismatch factor and gain of the probe on the UAV in the direction of the antenna. For convenience of notation we combine the latter three terms, which are usually described individually, in a single gain factor γ_p. The gain of the pth antenna, G_p depends on the positions of the antenna and the UAV, since the element radiation pattern is direction dependent. The voltage that we measure is further modified by the LNA and analog receiver path, which we describe by g_p. The voltage measured on the pth receiver path can thus be described by the Friis equation

$$v_p(\mathbf{x}_{\mathrm{UAV}}, t) = g_p G_p(\mathbf{x}_{\mathrm{UAV}}) \gamma_p(\mathbf{x}_{\mathrm{UAV}}) \times \exp\left\{\frac{2\pi \mathrm{j}}{\lambda} \|\mathbf{x}_{\mathrm{UAV}} - \mathbf{x}_p\|\right\} s(t) + n_p(t), \quad (1)$$

where $n_p(t)$ represents the noise on the measurements.

The signal transmitted by the UAV is usually not locked with the frequency reference of the device measuring the

signal at the output of the antenna. This precludes direct measurement of the transfer function between the probe and the AUT. We therefore need to determine the amplitude and phase differences between signal paths by correlating these signals, which provides a measure of the expected value

$$R_{p_1,p_2}\left(\mathbf{x}_{\mathrm{UAV}}\right) = \mathcal{E}\left\{v_{p_1}\left(\mathbf{x}_{\mathrm{UAV}},t\right)\overline{v_{p_2}}\left(\mathbf{x}_{\mathrm{UAV}},t\right)\right\}. \quad (2)$$

For ergodic signals, this permits us to simplify our description to a frequency domain only description. Based on the data model given in (1), we find

$$\begin{aligned} R_{p_1,p_2}\left(\mathbf{x}_{\mathrm{UAV}}\right) &= g_{p_1}\overline{g_{p_2}}G_{p_1}\left(\mathbf{x}_{\mathrm{UAV}}\right)\overline{G_{p_2}}\left(\mathbf{x}_{\mathrm{UAV}}\right) \\ &\times\gamma_{p_1}\left(\mathbf{x}_{\mathrm{UAV}}\right)\gamma_{p_2}\left(\mathbf{x}_{\mathrm{UAV}}\right)\sigma \\ &\times\exp\left\{\frac{2\pi\mathrm{j}}{\lambda}\left(\left\|\mathbf{x}_{\mathrm{UAV}}-\mathbf{x}_{p_1}\right\|-\left\|\mathbf{x}_{\mathrm{UAV}}-\mathbf{x}_{p_2}\right\|\right)\right\}, \end{aligned} \quad (3)$$

where σ is the power transmitted by the probe.

III. Proposed calibration procedure

A. Antenna position estimation

Our proposed method is an adaptation of (part of) the array calibration method described in [7], [8], which we modify to work with a near field source. Before we can calculate the path loss to the pth antenna γ_p and determine its radiation pattern G_p, we need to know its position. Based on experience from LOFAR, we may conclude that phase effects introduced by differences between element radiation patterns are reasonably small and can be averaged out over measurements in multiple directions. If we probe a sufficient number of directions, we can therefore ignore the effect of G_p and γ_p on the phase of R_{p_1,p_2}, which can therefore be described as

$$\angle R_{p_1,p_2} = \varphi_{p_1}-\varphi_{p_2}+\frac{2\pi}{\lambda}\left(\left\|\mathbf{x}_{\mathrm{UAV}}-\mathbf{x}_{p_1}\right\|-\left\|\mathbf{x}_{\mathrm{UAV}}-\mathbf{x}_{p_2}\right\|\right), \quad (4)$$

where $\varphi_p = \angle g_p$.

Since the antennas are positioned according to a designed configuration, we can describe the position of the pth antenna $\mathbf{x}_p$ as the sum of its nominal position $\mathbf{x}_p^0$ according to the designed configuration and an error introduced by the roll-out process $\boldsymbol{\epsilon}_p$. For convenience of notation, we introduce $\boldsymbol{\delta}_p = \mathbf{x}_{\mathrm{UAV}} - \mathbf{x}_p^0$. We can now write Eq. (4) as

$$\angle R_{p_1,p_2} = \varphi_{p_1} - \varphi_{p_2} + \frac{2\pi}{\lambda}\left(\left\|\boldsymbol{\delta}_{p_1}-\boldsymbol{\epsilon}_{p_1}\right\|-\left\|\boldsymbol{\delta}_{p_2}-\boldsymbol{\epsilon}_{p_2}\right\|\right). \quad (5)$$

Assuming that $\boldsymbol{\epsilon}_p << \boldsymbol{\delta}_p$, we can use the approximation

$$\begin{aligned} \left\|\boldsymbol{\delta}_p-\boldsymbol{\epsilon}_p\right\| &= \sqrt{\left\|\boldsymbol{\delta}_p\right\|^2+\left\|\boldsymbol{\epsilon}_p\right\|^2-2\boldsymbol{\delta}_p\cdot\boldsymbol{\epsilon}_p} \\ &\approx \sqrt{\left\|\boldsymbol{\delta}_p\right\|^2-2\boldsymbol{\delta}_p\cdot\boldsymbol{\epsilon}_p} \\ &= \left\|\boldsymbol{\delta}_p\right\|\sqrt{1-2\frac{\boldsymbol{\delta}_p\cdot\boldsymbol{\epsilon}_p}{\left\|\boldsymbol{\delta}_p\right\|^2}} \\ &\approx \left\|\boldsymbol{\delta}_p\right\|-\frac{\boldsymbol{\delta}_p\cdot\boldsymbol{\epsilon}_p}{\left\|\boldsymbol{\delta}_p\right\|}. \end{aligned}$$

Hence

$$\begin{aligned} \angle R_{p_1,p_2} &= \frac{2\pi}{\lambda}\left(\left\|\boldsymbol{\delta}_{p_1}\right\|-\left\|\boldsymbol{\delta}_{p_2}\right\|\right)+\left(\varphi_{p_1}-\varphi_{p_2}\right)+ \\ &\frac{2\pi}{\lambda}\left(-\frac{\boldsymbol{\delta}_{p_1}\cdot\boldsymbol{\epsilon}_{p_1}}{\left\|\boldsymbol{\delta}_{p_1}\right\|}+\frac{\boldsymbol{\delta}_{p_2}\cdot\boldsymbol{\epsilon}_{p_2}}{\left\|\boldsymbol{\delta}_{p_2}\right\|}\right). \end{aligned} \quad (6)$$

Since $\boldsymbol{\delta}_p$ only depends on the known position of the UAV and the known nominal position of the pth antenna, the first term can, in principle, be computed and subtracted. However, it is better to modify R_{p_1,p_2} using appropriate phasors to avoid issues with 2π phase ambiguities. We therefore introduce the modified array covariance matrix element

$$\widetilde{R}_{p_1,p_2} = \exp\left\{-\frac{2\pi\mathrm{j}}{\lambda}\left(\left\|\boldsymbol{\delta}_{p_1}\right\|-\left\|\boldsymbol{\delta}_{p_2}\right\|\right)\right\}R_{p_1,p_2}. \quad (7)$$

Assuming that the antennas are positioned in the (x,y)-plane such that their z-position is already known (just for convenience of notation, our method can easily be generalized to three dimensions), we have $\boldsymbol{\epsilon}_p = \left[\epsilon_{\mathrm{x},p},\epsilon_{\mathrm{y},p},0\right]^T$. Similarly, we have $\boldsymbol{\delta}_p = \left[\delta_{\mathrm{x},p},\delta_{\mathrm{y},p},\delta_{\mathrm{z},p}\right]^T$. Defining $\boldsymbol{\epsilon}_{\mathrm{x}} = \left[\epsilon_{\mathrm{x},1},\cdots\epsilon_{\mathrm{x},P}\right]^T$, $\boldsymbol{\epsilon}_{\mathrm{y}} = \left[\epsilon_{\mathrm{y},1},\cdots\epsilon_{\mathrm{y},P}\right]^T$ and $\boldsymbol{\varphi} = \left[\varphi_1,\cdots,\varphi_P\right]^T$, we can write

$$\begin{aligned} \angle\widetilde{R}_{p_1,p_2} &= \frac{2\pi}{\lambda}\left(-\frac{\delta_{\mathrm{x},p_1}\mathbf{e}_{p_1}}{\left\|\boldsymbol{\delta}_{p_1}\right\|}+\frac{\delta_{\mathrm{x},p_2}\mathbf{e}_{p_2}}{\left\|\boldsymbol{\delta}_{p_2}\right\|}\right)\boldsymbol{\epsilon}_{\mathrm{x}}+ \\ &\frac{2\pi}{\lambda}\left(-\frac{\delta_{\mathrm{y},p_1}\mathbf{e}_{p_1}}{\left\|\boldsymbol{\delta}_{p_1}\right\|}+\frac{\delta_{\mathrm{y},p_2}\mathbf{e}_{p_2}}{\left\|\boldsymbol{\delta}_{p_2}\right\|}\right)\boldsymbol{\epsilon}_{\mathrm{y}}+ \\ &\left(\mathbf{e}_{p_1}-\mathbf{e}_{p_2}\right)\boldsymbol{\varphi} \\ &= \mathbf{m}_{p_1,p_2}^T\left[\boldsymbol{\varphi}^T,\boldsymbol{\epsilon}_{\mathrm{x}}^T,\boldsymbol{\epsilon}_{\mathrm{y}}^T\right]^T, \end{aligned} \quad (8)$$

where $\mathbf{e}_p$ denotes the unit vector with all elements equal to zero except for its pth element, which is equal to unity. The unit vector $\mathbf{e}_p$ has length P, where P is the number of antennas in the array.

By stacking all measured phases $\angle\widetilde{R}_{p_1,p_2}$ in a vector $\boldsymbol{\phi}$ for all UAV positions and all antenna pairs and by stacking the corresponding row vectors $\mathbf{m}_{p_1,p_2}^T$ in a measurement matrix $\mathbf{M}$, we can build the system of equations

$$\boldsymbol{\phi} = \mathbf{M}\left[\boldsymbol{\varphi}^T,\boldsymbol{\epsilon}_{\mathrm{x}}^T,\boldsymbol{\epsilon}_{\mathrm{y}}^T\right]^T. \quad (9)$$

For K different UAV positions and an array of P antennas, $\boldsymbol{\phi}$ is a real valued vector with length P^2K and the measurement matrix $\mathbf{M}$ has size $P^2K\times 3P$. Since our measurements are insensitive to a common phase offset (phase referencing problem), the measurement matrix will always have a rank deficiency of 1, so it cannot be inverted. This can be solved by setting $\varphi_1 = 0$, making the first element in the array the phase reference. Mathematically, this means that we define the parameter vector $\boldsymbol{\theta}$ as

$$\boldsymbol{\theta} = \left[\varphi_2,\cdots,\varphi_P,\boldsymbol{\epsilon}_{\mathrm{x}}^T,\boldsymbol{\epsilon}_{\mathrm{y}}^T\right]^T \quad (10)$$

and use the modified measurement matrix $\widetilde{\mathbf{M}}$, which is equal to $\mathbf{M}$ with its first column removed (and therefore has size $P^2K\times(3P-1)$). Our antenna position and receiver path

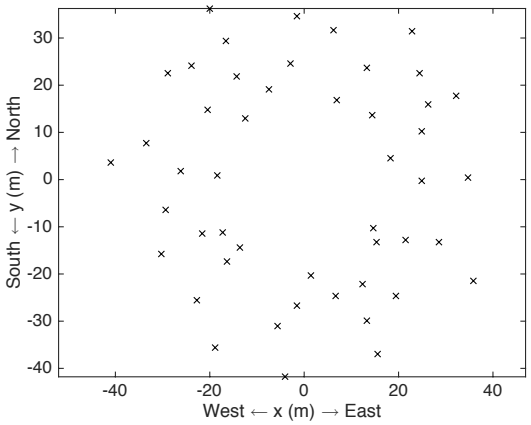

Fig. 1: Nominal antenna positions.

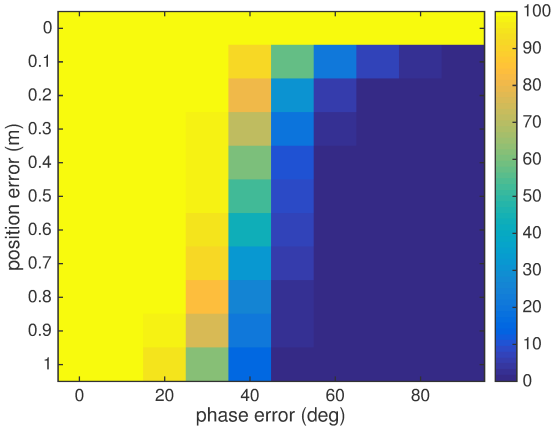

Fig. 2: Probability of successful reconstruction for different magnitudes of the rms phase and position errors.

phase calibration problem can thus be formulated as the least squares problem

$$\widehat{\boldsymbol{\theta}} = \underset{\boldsymbol{\theta}}{\operatorname{argmin}} \left\| \boldsymbol{\phi} - \widetilde{\mathbf{M}}\boldsymbol{\theta} \right\|^2, \tag{11}$$

which is readily solved using the Moore-Penrose pseudo-inverse, giving

$$\widehat{\boldsymbol{\theta}} = \left(\widetilde{\mathbf{M}}^H \widetilde{\mathbf{M}} \right)^{-1} \widetilde{\mathbf{M}}^H \boldsymbol{\phi}. \tag{12}$$

B. Radiation pattern measurement

Once the antenna positions have been estimated, we can calculate $\|\mathbf{x}_{\mathrm{UAV}} - \mathbf{x}_p\|$ and therefore the phase of the signal from the probe received at each antenna as well as the path loss towards each antenna. This only leaves the complex receiver path gains g_{p_1} and g_{p_2} and the element radiation patterns G_{p_1} and G_{p_2} as the only unknowns in Eq. (3). Since the amplitude of the receiver path gains (their phases are already obtained in the process described in the previous section) can be absorbed in the gain of the element radiation pattern, our system characterization problem has now been reduced to an element radiation pattern measurement problem. Such a problem can be effectively solved with UAV measurements as demonstrated in [5], [6].

IV. Simulations

To assess the method for position estimation outlined in the previous section, we simulated measurements on a 48-antenna LOFAR station. The nominal antenna positions are shown in Fig. 1. The UAV was assumed to follow a circular path with a radius of 25 m centred above the centre of the array at an altitude of 100 m. Measurements were done at 10 equally spaced points along this path at 50 MHz. Since we are primarily interested in the robustness of the proposed method and we may assume that the SNR of practical measurements is sufficiently high to ignore the effect of noise on the measurements, we generated noise free data.

To explore the performance of the proposed method for a range of phase and position errors, we did a series of Monte Carlo simulations, each consisting of 1000 runs. For each simulation, antenna gain phases and antenna position errors were randomly generated. The magnitude of these errors were varied from 0° to 90° in steps of 10° for the rms phase errors and 0 m to 1 m in steps of 0.1 m for the rms errors on the x- as well as the y-positions.

The procedure outlined in the previous section may still be sensitive to 2π phase ambiguities between the predicted and the measured phases. This may cause problems when the phase and position errors are large. Fig. 2 shows the probability of successful reconstruction for different combinations of phase and position errors. Given the fact that 1 m rms position error is a very significant deviation from the planned configuration, we can conclude that up to rms phase errors of about 40° the method works very well. Fig. 2 was created by comparison of the true position errors with the estimated position errors. In reality, we do not know the true position errors. Fortunately, the position error estimates degrade very quickly, leading to very large values that are easily recognised as being erroneous even if the ground truth is not known.

These 2π phase ambiguities emerge when we determine the angle from the measured value. The phase model described by Eq. (8) provides phases on a continuous scale, i.e., without 2π jumps. This problem can be circumvented by tracking the phases continuously during the flight of the UAV, such that the measured phases can be unwrapped. This can easily be achieved in practice as demonstrated by the measurements described in [6], which were taken at a 50 ms cadence while the UAV was flying at a speed of 1.5 m/s, which translates to a movement of 7.5 cm. Taking a conservative approach, this would allow us to phase unwrap for all measurements with $\lambda > 30$ cm, i.e., at frequencies lower than 1 GHz.

We have verified this conjecture by modifying our simulations such that the phases were tracked and unwrapped. In this modified simulation, the UAV was assumed to follow a circular path with a radius of 50 m centred above the centre of the array at an altitude of 100 m. Measurements

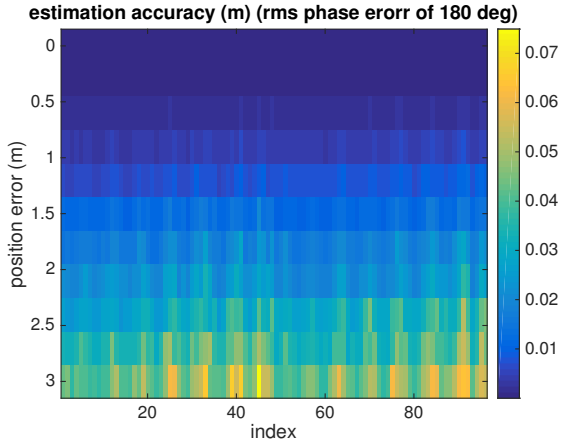

Fig. 3: Estimation accuracy for each of the elements in the parameter vector $\left[\boldsymbol{\epsilon}_{\mathrm{x}}^T, \boldsymbol{\epsilon}_{\mathrm{y}}^T\right]^T$ as function of the rms variation of the antenna positions for rms phase errors of 180 degrees.

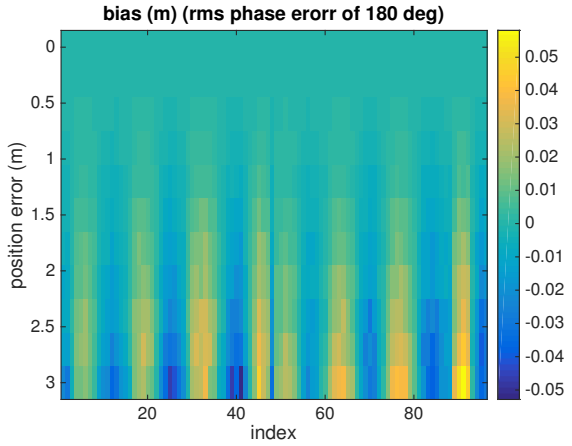

Fig. 4: Bias in the estimation of the elements of the parameter vector $\left[\boldsymbol{\epsilon}_{\mathrm{x}}^T, \boldsymbol{\epsilon}_{\mathrm{y}}^T\right]^T$ as function of the rms variation of the antenna positions for rms phase errors of 180 degrees.

were done continuously to allow phase unwrapping at 50 MHz. For estimation, 10 equally spaces points along the path were taken after phase unwrapping. With this setup, we did a series of Monte Carlo simulations consisting of 100 runs each. Antenna gain phases and antenna position errors were generated randomly as before, but their magnitude now varied from 0° to 360° in steps of 20° for the rms phase errors and 0 m to 3 m in steps of 0.3 m for the rms errors on the x- as well as the y-positions. We found that the proposed phase unwrapping procedure for the measured values allows 100% successful reconstruction for at least the indicated range of position and phase errors.

The proposed measurement linearises the phase model by assuming that $\boldsymbol{\epsilon}_p << \boldsymbol{\delta}_p$. This assumption introduces systematic deviations of the linearised phase model from the actually measured phases, so we need to verify that this does not lead to large estimation errors or biased estimates. Fig. 3 therefore shows the estimation accuracy obtained from the modified simulation (with phase unwrapping) for the parameter vector $\left[\boldsymbol{\epsilon}_{\mathrm{x}}^T, \boldsymbol{\epsilon}_{\mathrm{y}}^T\right]^T$ as function of rms variation of the antenna positions, while Fig. 4 shows the bias in the corresponding estimates. We see that the position estimation errors are more than a factor 10 smaller than the deviations from their nominal positions. This indicates that, if more accuracy is needed, we can start an iterative process to improve the accuracy of the position estimates to the required level. In Fig. 4 we see systematic variations, but these features are smaller than the estimation accuracy. We therefore conclude that, within the accuracy provided by the proposed method, it is unbiased.

V. Conclusions

In this paper, we proposed a method to calibrate the positions and element radiation patterns of the antennas in a low frequency aperture array station using a probe mounted on an UAV flying in the near field for the array. We validated this procedure using simulations demonstrating that the proposed method gives accurate and unbiased results if the measured phases can be unwrapped. Based on the measurements described in [6], this is feasible below frequencies of about 1 GHz. This makes the proposed method very suitable for SKA-low. This provides room to relax the requirements on antenna placement accuracy, which could potentially lead to large cost savings during the roll out of the SKA-low system.

In future work, we will also investigate optimum scanning strategies to maximise the probability of successful reconstruction with larger phase and position errors and robustness to measurement noise. We will also plan to validate our method by in-situ measurements on a LOFAR station.

Acknowledgment

This work is part of the SKA-TSM project and supported by The Northern Netherlands Provinces Alliance (SNN), Koers Noord and the Province of Drenthe. This work has also been partially supported by INAF through the TECNO INAF 2014 project entitled “Advanced calibration techniques for next generation low-frequency radio astronomical arrays”.

References

[1] P. E. Dewdney, P. J. Hall, R. T. Schilizzi, and T. J. L. W. Lazio, “The Square Kilometre Array,” *Proceedings of the IEEE*, vol. 97, no. 8, pp. 1483–1496, Aug. 2009.

[2] P. Dewdney *et al.*, “SKA1 System Baseline v2 Description,” SKA Office, Manchester (UK), Tech. Rep. SKA-TEL-SKO-0000308, 4 Nov. 2015.

[3] M. P. van Haarlem *et al.*, “LOFAR: The Low Frequency Array,” *Astronomy & Astrophysics*, vol. 556, no. A2, pp. 1–53, Aug. 2013.

[4] C. J. Lonsdale *et al.*, “The Murchison Widefield Array: Design Overview,” *Proceedings of the IEEE*, no. 8, pp. 1497–1506, Aug. 2009.

[5] G. Virone *et al.*, “Antenna Pattern Verification System Based on a Micro Unmanned Aerial Vehicle (UAV),” *IEEE Antennas and Wireless Propagation Letters*, vol. 13, pp. 169–172, 2014.

[6] G. Pupillo *et al.*, “Medicina array demonstrator: calibration and radiation pattern characterization using a UAV-mounted radio-frequency source,” *Experimental Astronomy*, vol. 39, no. 2, pp. 405–421, 2015.

[7] N. Fistas and A. Manikas, “A new general glabal array calibration method,” in *IEEE International Conference on Acoustics, Speech and Signal Processing*, vol. 4, 19–22 Apr. 1994, pp. 73–76.

[8] B. P. Flanagan and K. L. Bell, “Array self-calibration with large sensor position errors,” *Signal Processing*, vol. 81, no. 10, pp. 2201–2214, Oct. 2001.